Improved Tensor Current Limit from ^{8}B β Decay Including New Recoil-Order Calculations

B. Longfellow,[1] A. T. Gallant,[1] G. H. Sargsyan,[1,*] M. T. Burkey,[1] T. Y. Hirsh,[2] G. Savard,[3,4] N. D. Scielzo,[1]
L. Varriano,[3,4,†] M. Brodeur,[5] D. P. Burdette,[3,5] J. A. Clark,[3] D. Lascar,[3,6] K. D. Launey,[7] P. Mueller,[3] D. Ray,[3,8,‡]
K. S. Sharma,[8] A. A. Valverde,[3,8] G. L. Wilson,[7] and X. L. Yan[3]

[1]*Lawrence Livermore National Laboratory, Livermore, California 94550, USA*
[2]*Soreq Nuclear Research Center, Yavne 81800, Israel*
[3]*Physics Division, Argonne National Laboratory, Argonne, Illinois 60439, USA*
[4]*Department of Physics, University of Chicago, Chicago, Illinois 60637, USA*
[5]*Department of Physics and Astronomy, University of Notre Dame, Notre Dame, Indiana 46556, USA*
[6]*Department of Physics and Astronomy, Northwestern University, Evanston, Illinois 60208, USA*
[7]*Department of Physics and Astronomy, Louisiana State University, Baton Rouge, Louisiana 70803, USA*
[8]*Department of Physics and Astronomy, University of Manitoba, Winnipeg, Manitoba R3T 2N2, Canada*

A precision measurement of the β^+ decay of ^{8}B was performed using the Beta-decay Paul Trap to determine the β-ν angular correlation coefficient $a_{\beta\nu}$. The experimental results were combined with new *ab initio* symmetry-adapted no-core shell-model calculations to yield the second-most precise measurement from Gamow-Teller decays, $a_{\beta\nu} = -0.3345 \pm 0.0019_{\text{stat}} \pm 0.0021_{\text{syst}}$. This value agrees with the standard model value of $-1/3$ and improves uncertainties in ^{8}B by nearly a factor of 2. By combining results from ^{8}B and ^{8}Li, a tight limit on tensor current coupling to right-handed neutrinos was obtained. A recent global evaluation of all other precision β decay studies suggested a nonzero value for right-handed neutrino coupling in contradiction with the standard model at just above 3σ. The present results are of comparable sensitivity and do not support this finding.

Introduction.—The electroweak interaction can be written generally using parity-even C_i and parity-odd C_i' coupling constants for each possible Lorentz-invariant interaction type i: scalar (S), vector (V), axial vector (A), tensor (T), and pseudoscalar (P). In allowed nuclear β decay, only S and V interactions enter into Fermi transitions while only A and T interactions contribute to Gamow-Teller transitions. In the late 1950s and early 1960s, angular correlation measurements in β decay were key in establishing the standard model (SM) left-handed V-A nature of the electroweak interaction [1–3]. More recently, beyond-SM extensions have been proposed, such as leptoquark exchanges, contact interactions, and supersymmetry, that can manifest as non-SM couplings [4,5]. These exotic S and T currents can be probed by measuring small deviations from the expected β-ν correlation coefficient $a_{\beta\nu}$ values of $+1$ for pure Fermi (V) and $-1/3$ for pure Gamow-Teller (A) decays [6,7].

In the most recent global evaluation of precision β decay studies from 2021, the limits on a left-handed tensor coupling were consistent with the SM while a right-handed tensor coupling showed a 3.2σ deviation from zero [7]. This anomaly is predominantly driven by the $a_{\beta\nu}$ spectrometer *a*SPECT measurement of $a_{\beta\nu}$ in free neutron decay [8]. However, a 1.8σ discrepancy remains when excluding this result [7]. Measurements at the Large Hadron Collider and

of radiative pion decay also provide limits on tensor currents that are comparable and, in some cases, more stringent but are at substantially different energy scales [7,9,10]. Consequently, further high-precision measurements of $a_{\beta\nu}$ in additional systems are greatly desired.

In 2022, an ion trap measurement of ^{8}Li β^- decay obtained $a_{\beta\nu} = -0.3325(23)$ [11] providing the most stringent tensor current limit from a single measurement, the first improvement in nearly 60 years [3]. *Ab initio* symmetry-adapted no-core shell model (SA-NCSM) calculations of the recoil-order form factors in ^{8}Li β^- decay and their correlations with the ^{8}Li quadrupole moment were vital in greatly reducing systematic uncertainties [11,12]. Additionally, the first precision measurement of angular correlations in ^{8}B β^+ decay was recently performed yielding $a_{\beta\nu} = -0.3365(52)$ [13]. Since the signs of the Fierz interference term b_F [6] and some recoil-order terms [14] are different for β^- and β^+ decay, combining the results for ^{8}Li and ^{8}B gave strong constraints in (C_T, C_T') space [13]. However, SA-NCSM calculations like those for ^{8}Li were not available for ^{8}B leaving the recoil-order systematic uncertainty dominant [13].

In this Letter, we report a high-precision measurement of $a_{\beta\nu}$ in ^{8}B β^+ decay using the Beta-decay Paul Trap

(BPT) [15]. This Letter builds on our previous studies of ^{8}Li β^- decay [11,16,17] and improves the statistical uncertainty on our first ^{8}B measurement [13] by a factor of 2. Furthermore, the crucial large-scale SA-NCSM calculations for ^{8}B β^+ decay needed to significantly improve recoil-order systematics were performed. By combining the results for ^{8}B and ^{8}Li, a stringent limit on a right-handed coupling consistent with the SM was achieved. This result, of comparable precision to Ref. [7], will help resolve the current tension with the SM.

^{8}B β^+ decay predominantly proceeds via a nearly pure [18] Gamow-Teller transition from the $J^\pi = 2^+$, isospin $T = 1$ ^{8}B ground state to the broad $J^\pi = 2^+$, $T = 0$ resonance in ^{8}Be at 3 MeV which immediately breaks into two α particles. Since the β decay Q value is large and the mass is small, the considerable ^{8}Be* recoil leads to a maximum laboratory-frame energy difference for the α particles of about 450 keV. The α energy difference spectrum can be used to determine $a_{\beta\nu}$ [19]. The decay rate for β-delayed α emission from an unpolarized nucleus can be expressed to leading order as [14]

$$W \propto F(\pm Z, E_e) p_e E_e (E_0 - E)^2$$
$$\times \left[g_1 \pm \sqrt{1 - (Z\alpha_{FS})^2} \, b_F \frac{m_e}{E_e} + g_2 \frac{\vec{p}_e \cdot \vec{p}_\nu}{E_e E_\nu} \right.$$
$$\left. + \frac{\tau_{J',J''}(L)}{10} g_{12} \left(\frac{(\vec{p}_e \cdot \hat{p}_\alpha)(\vec{p}_\nu \cdot \hat{p}_\alpha)}{E_e E_\nu} - \frac{1}{3} \frac{\vec{p}_e \cdot \vec{p}_\nu}{E_e E_\nu} \right) \right] \quad (1)$$

where the upper (lower) signs correspond to β^- (β^+) decay. Here, $F(\pm Z, E_e)$ is the Fermi function, $(E_e, \vec{p}_e)$ and $(E_\nu, \vec{p}_\nu)$ are the β and ν four-momenta, E_0 is the decay endpoint energy, m_e is the electron mass, $\hat{p}_\alpha$ is the direction of the delayed α, Z is the atomic number of the daughter nucleus, and α_{FS} is the fine structure constant. The coefficient $\tau_{J',J''}(L)$ depends on the spin sequence of the decay $J \to J' \to J''$ and the angular momentum L of the α relative to the daughter. For ^{8}B and ^{8}Li β decay, the spin sequence is $2^+ \to 2^+ \to 0^+$ with $L = 2$ and $\tau = 10$ [14]. The spectral functions g_1, g_2, and g_{12} depend mainly on the coupling constants C_i and C_i'. In the SM, $g_1 = 1$, $g_2 = -1/3$, and $g_{12} = -1$. The β-ν correlation coefficient $a_{\beta\nu}$ is defined as g_2/g_1. When the delayed α is emitted parallel to the β the effective value of $a_{\beta\nu}$ becomes $[g_2 + (2/3)g_{12}]/g_1$ effectively tripling the correlation $(g_2/g_1 = -1/3$ and $[g_2 + (2/3)g_{12}]/g_1 = -1)$. Conversely, when the α is emitted perpendicular to the β, the effective value is $[g_2 - (1/3)g_{12}]/g_1 = 0$, suppressing the correlation.

Additional corrections to the spectral functions enter at recoil order depending on E_e/m_e, E_0/m_e, and the recoil-order form factors b_{WM} (weak magnetism), d (induced tensor), and j_2 and j_3 (second-forbidden axial vectors), causing additional correlations between the decay products. We used the SA-NCSM [20–22] to calculate recoil-order form factors, reported as fractions over the Gamow-Teller

matrix element (c_0) and factors of the mass number (A). For these calculations, we adopted various chiral potentials without renormalization in nuclear medium: N^{3}LO-EM [23], NNLO$_{opt}$ [24], and NNLO$_{sat}$ [25], and in addition, the soft JISP16 phase-equivalent NN interaction [26]. The ^{8}Be resonances from SA-NCSM calculations are discussed in subsections C and D of the Supplemental Material of Ref. [12].

In Fig. 1, each marker corresponds to one calculation with a specific model space and harmonic oscillator spacing $\hbar\Omega$ using a potential mentioned above. The values of j_2/A^2c_0 and j_3/A^2c_0 for the transition to the ^{8}Be 2_1^+ state were predicted using the linear correlation between the calculated j_2/A^2c_0 and j_3/A^2c_0 values and the calculated ^{8}B ground state quadrupole moments $Q(2_{g.s.}^+)$ compared to the experimentally measured value [6.43(14) e fm^2] [27]. For about one-third of the points, the prescription in Ref. [28] was used to accommodate large model spaces, clustering, and collectivity. Excluding the SA calculations would slightly decrease the linear regression uncertainty discussed below. The same procedure was used to predict d/Ac_0 to the ^{8}Be 2_1^+ state. For b_{WM}/Ac_0 to all states in ^{8}Be and for the other recoil-order terms to higher-lying 2^+ states, the values were calculated using NNLO$_{opt}$ and JISP16 with uncertainties from varying $\hbar\Omega$ from 20 MeV by ± 5 MeV and model-space sizes from $N_{max} = 6$–12.

The total uncertainties on j_2/A^2c_0, j_3/A^2c_0, and d/Ac_0 in Table I for ^{8}B β^+ decay to the ^{8}Be 2_1^+ state arise from two parts added in quadrature: the $Q(2_{g.s.}^+)$ experimental uncertainty [6.43(14) e fm^2 [27]] intersecting with the linear
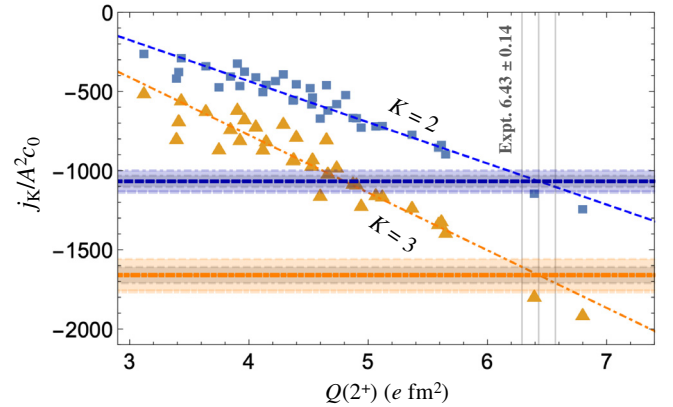

FIG. 1. Correlations between the calculated ^{8}B $Q(2_{g.s.}^+)$ and the calculated values of j_2/A^2c_0 (squares) and j_3/A^2c_0 (triangles) for ^{8}B β^+ decay to the ^{8}Be 2_1^+ using various interactions and model spaces. The vertical gray lines show the experimental value of ^{8}B $Q(2_{g.s.}^+)$ with uncertainties [27]. The intersections with the $K = 2$ and $K = 3$ best fit lines give the predictions for j_2/A^2c_0 and j_3/A^2c_0, respectively. The darker horizontal bands are uncertainties solely from the $Q(2_{g.s.}^+)$ experimental uncertainty while the lighter bands also include the linear regression uncertainty.

TABLE I. Recoil-order terms from SA-NCSM for ^{8}B β^+ decay and ^{8}Li β^- decay [12]. Results for the 2_1^+ $j_{2,3}/A^2c_0$ and d/Ac_0 are based on correlations to $Q(2_{\text{g.s.}}^+)$; all other values use NNLO$_{\text{opt}}$ and JISP16 with uncertainties from variations in $\hbar\Omega$ and model-space size.

		j_2/A^2c_0	j_3/A^2c_0	d/Ac_0	b_{WM}/Ac_0
^{8}B	2_1^+	$-1067(68)$	$-1660(102)$	$9.6(6)$	$6.1(5)$
	2_2^+ (intruder)	$10(45)$	$-41(75)$	$-0.5(8)$	$3.7(4)$
	2_3^+ (doublet 1)	$8(4)$	$-53(20)$	$0.1(1)$	$3.8(2)$
	2_4^+ (doublet 2)	$7(5)$	$-70(13)$	$0.2(1)$	$3.8(2)$
^{8}Li	2_1^+	$-966(36)$	$-1546(44)$	$10.0(10)$	$6.0(4)$
	2_2^+ (intruder)	$-10(10)$	$-80(30)$	$-0.5(5)$	$3.7(4)$
	2_3^+ (doublet 1)	$12(5)$	$-60(15)$	$0.3(2)$	$3.8(2)$
	2_4^+ (doublet 2)	$11(3)$	$-65(11)$	$0.2(2)$	$3.8(2)$

regression slope and the regression uncertainty from the Student's t distribution at 95% confidence level. The linear dependence is observed regardless of any errors that may arise from the many-body truncation and the various interactions used, including, for instance, the effect of SA model space selections, higher-order effects (e.g., Refs. [29,30]) associated with the different interactions, as well as effects from two-body currents in the operators for $Q(2_{\text{g.s.}}^+)$ [29] and for axial beta transitions [31,32]. Hence, given the variety of input, the regression provides uncertainty that is parameter and model (interaction) independent.

In Table I, the SA-NCSM recoil-order terms for ^{8}B β^+ decay and ^{8}Li β^- decay [12] are compared. While $Q(2_{\text{g.s.}}^+)$ for ^{8}B and ^{8}Li differ by over a factor of 2, the recoil-order terms from correlations are similar. The isospin-symmetry breaking realistic Hamiltonians yield b_{WM}/Ac_0 values for the mirror nuclei consistent within uncertainties (similarly for d/Ac_0), in agreement with the conserved vector current hypothesis [1]. As in Ref. [12], larger recoil-order terms to the 2_1^+ state than to the 16.626- and 16.922-MeV doublet states [33] and the experimentally unconfirmed "intruder" state are predicted. Compared to the uncertainties on $j_{2,3}/A^2c_0$ from Ref. [34], which provided the largest systematic uncertainties in the first ^{8}B experiment [13], the uncertainties for the 2_1^+ state are factors of 2.2 and 4.6 times more precise, respectively. Reference [12] discusses the differences between the present values of $j_{2,3}/A^2c_0$ and those in Ref. [34].

The present experiment was performed at Argonne National Laboratory using the ATLAS facility and is also described in Ref. [35]. The ^{8}B radioactive beam was produced via ^{6}Li(^{3}He, n)^{8}B. The reaction products were focused into a gas catcher using a large solenoid. The highly chemically reactive ^{8}B was incorporated into several molecules through interactions with contaminants with the highest activity at mass $A = 42$. Molecular effects on $a_{\beta\nu}$

are negligible [13,36]. The ion injection system [37] was used to thermalize, collect, bunch and transport the ions to the preparation gas-filled Penning trap [38] and the $A = 42$ beam was delivered to the BPT.

The BPT is a linear Paul trap consisting of four thin, segmented electrodes that confine ions in a small, localized volume allowing the decay products to emerge nearly scattering free. The trapping region was surrounded by four $64 \times 64 \times 1$ mm^3 double-sided silicon strip detectors (DSSDs) with both front and back sides segmented into 32 strips. The DSSDs were calibrated in situ using two ^{148}Gd and two ^{244}Cm spectroscopy-grade sources. Furthermore, the DSSD minimum ionizing β spectra were utilized as calibration points around 300 keV by matching to GEANT4 simulations benchmarked against cosmic-ray muons [39]. The edge strips and 17 other strips with poor energy resolution were excluded [35].

To exploit the enhancement in $a_{\beta\nu}$ for parallel α and β particles, the analysis was restricted to α-α-β triple coincidences where the two α particles struck opposite-facing DSSDs and the β struck the same detector as one α. Hits depositing between 200 and 700 keV were considered β particles and hits depositing more than 700 keV were considered α particles based on GEANT4 simulations of the α and β energy spectra. The α particles were required to have a time difference within 800 ns and the β was required to have a time difference within 4 μs of both α particles.

For each hit, the front and back strip energies were required to agree within 30 keV. Additionally, only events with one reconstructed α-α pair and one reconstructed β were considered to avoid ambiguity in selecting correct pairs. The α-α-β triple coincidence signature effectively eliminates background events. Events within 35 ms of the trap closing were discarded since opening the trap disturbs the ion cloud thermal equilibrium. To minimize complications from the possible "intruder" state, both α energies were required to be greater than 850 keV and the sum of the α energies was required to be less than 3.75 MeV to select a narrow energy region of about 1.7 to 3.75 MeV around the first 2^+ state in ^{8}Be. These are the same cuts used in the recent ^{8}Li measurement [11].

To fit the experimental data, a detailed model of the setup and high-fidelity simulations of the decay kinematics including electromagnetic [40], induced Coulomb [41], radiative [42], and recoil-order corrections [14] assuming pure A and T interactions were utilized. The Fermi function formulation was taken from Ref. [43], modified to the root-mean-square radius in Ref. [13]. The ^{8}Be* excitation energy spectrum was taken from Ref. [35]. The β particles were propagated through a GEANT4 model of the BPT geometry and surrounding infrastructure using the standard electromagnetic physics list "option3." The DSSD response was applied separately. The simulated data were passed through the same sortcode as the experimental data.

The experimental α energy difference spectrum for β particles "parallel" to the α particles is shown in
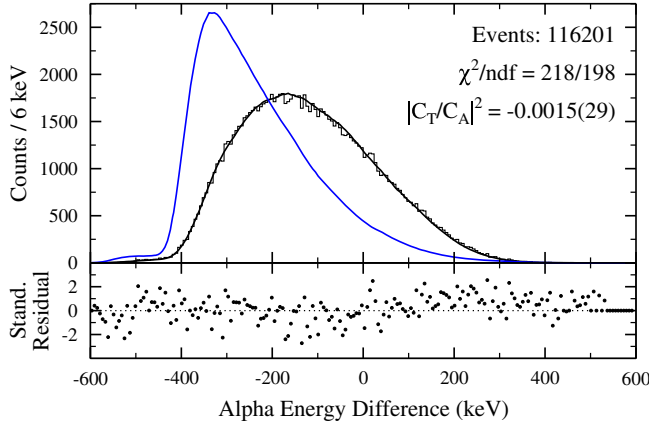
FIG. 2. Experimental α energy difference spectrum for β particles "parallel" to the α particles fit to a linear combination of pure A and T simulations (black curve) assuming the "intruder" state exists (see text). The pure T simulation is blue. The bottom panel shows the standardized residuals.

Fig. 2. The data were fit using maximum likelihood to a linear combination of pure A and T simulations. The ratio of the couplings $|C_T/C_A|^2$ and a normalization constant were the only parameters. The systematic uncertainties here are similar to Ref. [11] and are briefly discussed below and summarized in Table II.

Intruder state.—The experimentally unconfirmed "intruder" 2^+ state in the SA-NCSM calculations has different recoil-order terms than the doublet levels. If we assume the "intruder" state does not exist, the extracted value of $|C_T/C_A|^2$ with only statistical uncertainty is $-0.0019(29)$ while including the "intruder" state changes the value to $-0.0015(29)$. We therefore adopt $|C_T/C_A|^2 = -0.0017$ and a systematic uncertainty of 0.0002 added linearly to other systematics.

Recoil and radiative terms.—Varying the recoil-order terms in Table I by their uncertainties yielded a total uncertainty of 0.0020 with b_{WM}, d, j_2, and j_3 contributing about 0.0010, 0.0011, 0.0005, and 0.0013, respectively. The uncertainty from Z-independent radiative corrections [42] was 0.0007 giving a combined uncertainty from recoil

TABLE II. Dominant systematic uncertainties on $|C_T/C_A|^2$ at 1σ.

Source		Uncertainty
Theory	Intruder state[a]	0.0002
	Recoil and radiative terms	0.0021
Experiment	Energy calibration	0.0008
	Detector line shape	0.0010
	Data cuts	0.0011
	β scattering	0.0010
	Ion cloud size	0.0003
Total		0.0031

[a]Added linearly.

and radiative terms of 0.0021. This is larger than for ^{8}Li (0.0015) [11] due to the higher recoil-order term uncertainties. Nevertheless, the new SA-NSCM calculations lead to a factor of 2 improvement in recoil and radiative correction uncertainty compared to our first ^{8}B measurement [13] which used recoil-order values from Ref. [34].

Energy calibration.—The energy calibration accounted for detector dead layers, nonionizing energy loss, the pulse-height defect, and the α source thicknesses. Systematic uncertainties in the calibration are described in Refs. [35,39]. By varying the calibration within its total uncertainties, the uncertainty on $|C_T/C_A|^2$ was evaluated as 0.0008.

Detector line shape.—A DSSD line shape model was developed using spectroscopy-grade α sources and an α-beam detector characterization experiment. Aspects of the detector response including dead layer thicknesses for different DSSD features and charge sharing between front and back strips were varied leading to 0.0010 uncertainty on $|C_T/C_A|^2$.

Data cuts.—The front-back energy difference cut for α particles was varied from ± 30 keV [11] to the asymmetric -80 to 140 keV [35] which incorporates the satellite peak from back-strip charge sharing. In addition, the low bound for the α energy was changed from 850 to 700 keV and, separately, the high bound for the β energy was changed from 700 to 600 keV. Finally, the relative timing cuts and the cut to allow ion cloud cooling were doubled. Altogether, the uncertainty from these changes added in quadrature was 0.0011.

β scattering.—For "triples," about 20% of the β particles scatter before reaching a DSSD, affecting the angular correlations. If only simulated events without β scattering are used, $|C_T/C_A|^2$ would shift by about -0.0250. The GEANT4 simulations were benchmarked by comparing to the experimental "triples/doubles" ratio, the fraction of backscattered β particles, and the minimum-ionizing β energy spectrum. Following Refs. [11,13], the uncertainty on $|C_T/C_A|^2$ from β scattering modeling was evaluated as 0.0010 by varying the fraction of scattered events.

Ion cloud size.—The ^{8}B ion cloud was imaged [15] and found to be Gaussian distributed, extending 1.17 mm radially and 3.14 mm axially at 1σ. The ion cloud dimensions were varied by 5% leading to 0.0003 uncertainty on $|C_T/C_A|^2$.

In total, our result is $|C_T/C_A|^2 = -0.0017 \pm 0.0029_{\text{stat}} \pm 0.0031_{\text{syst}}$ at 1σ. In the fit we assume $C_T = -C_T'$ and $b_F = 0$ which gives $a_{\beta\nu} = -0.3345 \pm 0.0019_{\text{stat}} \pm 0.0021_{\text{syst}}$, consistent with the SM prediction of $-1/3$. The present value of $a_{\beta\nu} = -0.3345(28)$ is slightly more precise than the corrected ^{6}He measurement from 1963 of $a_{\beta\nu} = -0.3308(30)$ [3,42] making it the second-tightest constraint on tensor currents following the most recent ^{8}Li value of $a_{\beta\nu} = -0.3325(23)$ [11]. Compared to the first ^{8}B value of $a_{\beta\nu} = -0.3365(52)$ [13], the present measurement is 1.8 times more precise.
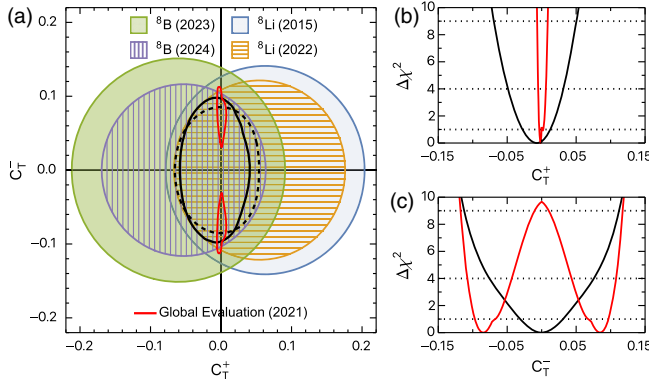
FIG. 3. (a) 95.5% confidence limit regions in (C_T^+, C_T^-) space for ^{8}Li (blue [17], orange [11]) and ^{8}B (green [13], purple [present]) along with the resulting joint probability distribution using an estimate of correlated systematics (solid black) and assuming uncorrelated uncertainties (dashed black). The global limits [7] (red) do not include the $A = 8$ results. The marginalized $\Delta\chi^2$ distributions for C_T^+ and C_T^- with correlations (black) are compared to Ref. [7] (including the updates in Ref. [46]) (red) in (b) and (c). The dotted horizontal lines at $\Delta\chi^2 + 1$, 4, 9 correspond to $1, 2, 3\sigma$.

A nonzero Fierz interference term can be included using $\tilde{a}_{\beta\nu} = a_{\beta\nu}/[1 \pm \sqrt{1 - (Z\alpha_{FS})^2} b_F \langle m_e/E_e \rangle]$ [44,45]. Here the upper (lower) signs correspond to β^- (β^+) decay. Accounting for experimental cuts, $\langle m_e/E_e \rangle$ is approximately 0.085 for ^{8}B in this Letter. To compare with the global results of Falkowski *et al.* [7], C_T and C_T' were rotated to the left-handed C_T^+ and right-handed C_T^- using $C_T = (C_T^+ + C_T^-)/2$ and $C_T' = (C_T^+ - C_T^-)/2$. Furthermore, the assumption $C_A = C_A'$ implies $C_A = C_A^+/2$ and $C_A^- = 0$. The value $C_A^+ = -1.2544$ [7] was utilized.

Similar to Ref. [13], probability distributions in (C_T^+, C_T^-) space were constructed using $\tilde{a}_{\beta\nu}$ for the ^{8}Li and ^{8}B results to provide stronger constraints due to the b_F sign change. A Monte Carlo approach was utilized to account for correlations in the systematic uncertainties between the ^{8}Li and ^{8}B BPT experiments. The correlation coefficient between the present work and Ref. [11], which used the same SA-NCSM approach for the recoil-order terms and benefited from the same setup improvements, was estimated as 0.9. Likewise, the correlation coefficient between the older experiments [13,17], which used the recoil-order terms from Ref. [34], was estimated as 0.9. The correlation coefficients between experiments in different generations were estimated as 0.25 largely due to the differences in the uncertainty-dominating recoil-order terms. Figure 3 shows the effect of correlations on the joint limit.

As seen in Fig. 3, the current global limits [7] (updated as described in Ref. [46]), which do not include the $A = 8$ results, strongly constrain C_T^+ but favor a nonzero C_T^- value to just above 3σ. The present joint limit is consistent with

the SM. For the differential spectra here, constraints found using $\tilde{a}$ are slightly conservative [47].

In summary, the Beta-decay Paul Trap was used to precisely measure the β-ν angular correlation coefficient in ^{8}B β^+ decay. New SA-NCSM calculations were performed to improve the systematic uncertainty from recoil-order corrections by a factor of 2. The present tensor current limit is the second-most stringent in the low-energy regime. The combined ^{8}B and ^{8}Li limit for right-handed coupling is competitive with the recent global evaluation of precision β decay data. Unlike the global evaluation, this Letter does not find a discrepancy with the SM.

*Present address: Facility for Rare Isotope Beams, Michigan State University, East Lansing, Michigan 48824, USA.
†Present address: Department of Physics and Center for Experimental Nuclear Physics and Astrophysics, University of Washington, Seattle, Washington 98195, USA.
‡Present address: TRIUMF, Vancouver, British Columbia V6T 2A3, Canada.

[1] R. P. Feynman and M. Gell-Mann, Phys. Rev. **109**, 193 (1958).
[2] E. C. G. Sudarshan and R. E. Marshak, Phys. Rev. **109**, 1860 (1958).
[3] C. H. Johnson, F. Pleasonton, and T. A. Carlson, Phys. Rev. **132**, 1149 (1963).
[4] P. Herczeg, Prog. Part. Nucl. Phys. **46**, 413 (2001).
[5] S. Profumo, M. J. Ramsey-Musolf, and S. Tulin, Phys. Rev. D **75**, 075017 (2007).
[6] J. D. Jackson, S. B. Treiman, and H. W. Wyld, Phys. Rev. **106**, 517 (1957).
[7] A. Falkowski, M. González-Alonso, and O. Naviliat-Cuncic, J. High Energy Phys. 04 (2021) 126.
[8] M. Beck, F. Ayala Guardia, M. Borg, J. Kahlenberg, R. Muñoz Horta, C. Schmidt, A. Wunderle, W. Heil, R. Maisonobe, M. Simson, T. Soldner, R. Virot, O. Zimmer,

M. Klopf, G. Konrad, S. Baeßler, F. Glück, and U. Schmidt, Phys. Rev. C **101**, 055506 (2020).

[9] M. Bychkov *et al.*, Phys. Rev. Lett. **103**, 051802 (2009).

[10] M. González-Alonso, O. Naviliat-Cuncic, and N. Severijns, Prog. Part. Nucl. Phys. **104**, 165 (2019).

[11] M. T. Burkey *et al.*, Phys. Rev. Lett. **128**, 202502 (2022).

[12] G. H. Sargsyan, K. D. Launey, M. T. Burkey, A. T. Gallant, N. D. Scielzo, G. Savard, A. Mercenne, T. Dytrych, D. Langr, L. Varriano, B. Longfellow, T. Y. Hirsh, and J. P. Draayer, Phys. Rev. Lett. **128**, 202503 (2022).

[13] A. T. Gallant *et al.*, Phys. Rev. Lett. **130**, 192502 (2023).

[14] B. R. Holstein, Rev. Mod. Phys. **46**, 789 (1974).

[15] N. D. Scielzo *et al.*, Nucl. Instrum. Methods Phys. Res., Sect. A **681**, 94 (2012).

[16] G. Li *et al.*, Phys. Rev. Lett. **110**, 092502 (2013).

[17] M. G. Sternberg *et al.*, Phys. Rev. Lett. **115**, 182501 (2015).

[18] R. B. Wiringa, S. Pastore, S. C. Pieper, and G. A. Miller, Phys. Rev. C **88**, 044333 (2013).

[19] R. D. MacFarlane, N. S. Oakey, and R. J. Nickles, Phys. Lett. **34B**, 133 (1971).

[20] K. D. Launey, T. Dytrych, and J. P. Draayer, Prog. Part. Nucl. Phys. **89**, 101 (2016).

[21] K. D. Launey, A. Mercenne, and T. Dytrych, Annu. Rev. Nucl. Part. Sci. **71** (2021).

[22] T. Dytrych, K. D. Launey, J. P. Draayer, D. J. Rowe, J. L. Wood, G. Rosensteel, C. Bahri, D. Langr, and R. B. Baker, Phys. Rev. Lett. **124**, 042501 (2020).

[23] D. R. Entem and R. Machleidt, Phys. Rev. C **68**, 041001(R) (2003).

[24] A. Ekström, G. Baardsen, C. Forssén, G. Hagen, M. Hjorth-Jensen, G. R. Jansen, R. Machleidt, W. Nazarewicz *et al.*, Phys. Rev. Lett. **110**, 192502 (2013).

[25] A. Ekström, G. R. Jansen, K. A. Wendt, G. Hagen, T. Papenbrock, B. D. Carlsson, C. Forssén, M. Hjorth-Jensen, P. Navrátil, and W. Nazarewicz, Phys. Rev. C **91**, 051301(R) (2015).

[26] A. M. Shirokov, J. P. Vary, A. I. Mazur, and T. A. Weber, Phys. Lett. B **644**, 33 (2007).

[27] T. Sumikama, T. Nagatomo, M. Ogura, T. Iwakoshi, Y. Nakashima, H. Fujiwara, K. Matsuta, T. Minamisono, M. Fukuda, and M. Mihara, Phys. Rev. C **74**, 024327 (2006).

[28] K. D. Launey, T. Dytrych, G. H. Sargsyan, R. B. Baker, and J. P. Draayer, Eur. Phys. J. Spec. Top. **229**, 2429 (2020).

[29] A. A. Filin, D. Möller, V. Baru, E. Epelbaum, H. Krebs, and P. Reinert, Phys. Rev. C **103**, 024313 (2021).

[30] P. Maris *et al.* (LENPIC Collaboration), Phys. Rev. C **103**, 054001 (2021).

[31] P. Gysbers, G. Hagen, J. D. Holt, G. R. Jansen, T. D. Morris, P. Navrátil, T. Papenbrock, S. Quaglioni, A. Schwenk, S. R. Stroberg, and K. A. Wendt, Nat. Phys. **15**, 428 (2019).

[32] G. B. King, L. Andreoli, S. Pastore, M. Piarulli, R. Schiavilla, R. B. Wiringa, J. Carlson, and S. Gandolfi, Phys. Rev. C **102**, 025501 (2020).

[33] F. Ajzenberg-Selove, Nucl. Phys. **A413**, 1 (1984).

[34] T. Sumikama, K. Matsuta, T. Nagatomo, M. Ogura, T. Iwakoshi, Y. Nakashima, H. Fujiwara, M. Fukuda, M. Mihara, K. Minamisono, T. Yamaguchi, and T. Minamisono, Phys. Rev. C **83**, 065501 (2011).

[35] B. Longfellow, A. T. Gallant, T. Y. Hirsh, M. T. Burkey, G. Savard, N. D. Scielzo, L. Varriano, M. Brodeur, D. P. Burdette, J. A. Clark, D. Lascar, P. Mueller, D. Ray, K. S. Sharma, A. A. Valverde, G. L. Wilson, and X. L. Yan, Phys. Rev. C **107**, L032801 (2023).

[36] L. Hayen, N. Severijns, K. Bodek, D. Rozpedzik, and X. Mougeot, Rev. Mod. Phys. **90**, 015008 (2018).

[37] J. Fallis, Ph.D. thesis, University of Manitoba, 2009.

[38] G. Savard, St. Becker, G. Bollen, H.-J. Kluge, R. B. Moore, Th. Otto, L. Schweikhard, H. Stolzenberg, and U. Wiess, Phys. Lett. A **158**, 247 (1991).

[39] T. Y. Hirsh *et al.*, Nucl. Instrum. Methods Phys. Res., Sect. A **887**, 122 (2018).

[40] F. P. Calaprice and B. R. Holstein, Nucl. Phys. **A273**, 301 (1976).

[41] B. R. Holstein, Phys. Rev. C **10**, 1215 (1974).

[42] F. Glück, Nucl. Phys. **A628**, 493 (1998).

[43] H. Behrens and J. Jänecke, in *Numerical Tables for Beta-Decay and Electron Capture*, edited by H. Schopper (Springer-Verlag, Berlin, 1969).

[44] H. Paul, Nucl. Phys. **A154**, 160 (1970).

[45] N. Severijns, M. Beck, and O. Naviliat-Cuncic, Rev. Mod. Phys. **78**, 991 (2006).

[46] V. Cirigliano, D. Díaz-Calderón, A. Falkowski, M. González-Alonso, and A. Rodríguez-Sánchez, J. High Energy Phys. 04 (2022) 152.

[47] M. González-Alonso and O. Naviliat-Cuncic, Phys. Rev. C **94**, 035503 (2016).